




Multi-Objective Optimal planning of Renewable Energy Sources & Electric Vehicle Charging Stations in Unbalanced Radial Distribution Systems using Harris Hawk Optimization Algorithm

Ponnam Venkata K. Babu*, K. Swarnasri*, P. Vijetha**

*Department of EEE, RVR & JC College of Engineering, Chowdavaram, Guntur 522006, A.P, India.

**Department of Chemical Engineering, VFSTR University, Vadlamudi, Guntur 522213, A.P, India.

(kishore.ponnam@gmail.com, swarnasrik@gmail.com, vijetha.ponnam@gmail.com)

†
Department of Chemical Engineering, VFSTR University, Vadlamudi, Guntur 522213, A.P, India, Tel: +91 9494414529,
vijetha.ponnam@gmail.com

Received: 16.12.2021 Accepted: 21.01.2022

Abstract- This paper aims to examine the effect of the electric vehicle charging station (EVCS) loads on an unbalanced radial distribution system (URDS) voltage profile and losses. Further, to determine the optimal placement of EVCSs & Distribution Generator (DG) for mitigating the losses & improving the voltage profile Harris Hawk Optimization (HHO) algorithm proposes. HHO is a widespread swarm-based, gradient-free optimization technique based on the supportive action & hunting characteristic of Harris hawks in nature with numerous energetic phases of exploration & exploitation. The active, reactive power limits and different operational constraints of URDS consider while minimizing the losses. It observed that the unbalanced radial distribution network could survive the deployment of EVCSs at the vital buses up to a certain extent. However, the allocation of EVCSs at the weak buses of the network prevents the power system's stable operation. The analysis performs on the IEEE 25 bus Unbalanced radial distribution network for the placement of EVCS & DG. In addition, HHO's superiority in terms of convergence characteristics compares to other modern heuristic algorithms.

Keywords- electric vehicle; charging station; distributed generator; optimal placement; Harris Hawk Optimization; unbalanced radial distribution system.

1. Introduction

Overuse of fossil fuels, such as crude oil and gas in the transportation sector, leads to a drastic increase in temperature and excessive carbon release, resulting in the degradation of the environment. Global warming impacts the atmosphere by erratic rains and increasing temperatures. Many countries are encouraging the transportation industry by promoting battery-fed vehicles to reduce the emissions in their region. Electrification can be effectively applied in the transport sector by developing a solid infrastructure for efficient charging stations for electric vehicles. Adding an EV charging station to the system will consume more power, impacting the bus voltage & thermal stability [1]. To overcome the challenges faced by the utility and the customer, the charging infrastructure requires optimal allocation of the electric vehicle charging stations, Distributed Generation units (DGs) in the distribution network and optimal scheduling of EVs charging.

Mohsenzadeh et al. [2] used a Genetic algorithm for optimal planning of plug-in electric vehicle parking lots at different levels to improve system reliability and minimize the power loss and voltage drop. The algorithm is tested on a 33-bus radial distribution system (RDS). Ramana et al. [3] presented a methodology based on voltage index analysis & variational algorithm for solving the best location and size of DG in URDS. The practicality of the proposed method is confirmed by applied on IEEE 25 & 37 node URDS test feeders. Janamala et al. [4] proposed a future search algorithm for determining the optimal allocation of DG & EV fleets concurrently by considering techno environmental aspects of RDS. Sanjay et al. [5] used a hybrid grey wolf optimization algorithm for optimal placement and DG size. This algorithm is employed on IEEE 33, 69 & Indian 85 bus RDS to minimize the losses. Quadri et al. [6] introduced a comprehensive teaching learning-based optimization (CTLBO) to optimize the allotment of distributed generators in radial distribution systems for power savings and network loss reduction. Kayalvizhi & Vinod [7] anticipated a hybrid Grid-based

Multi-objective Harmony Search technique for optimum location of DG in RDS. Ali Jabbarly & Hossein Shayeghi [8] proposed a firefly nonlinear innovative algorithm to optimize a distribution network's technical & financial indexes in the existence of different types of DGs. With the migration to PHVs, the electric grid's limits, such as voltage constraints, losses are examined for a practical RDS in Ontario, Canada [9]. Modelling EVCS in an RDS can be used to investigate the consequence of EVCS on the electrical grid [10]. EVCS does not charge EVs the entire day, which is more involved during peak hours & planned according to the user's needs. These preliminary charging stations (CS) schedules in the RDS influence the power grid is easily assessed [11]. Using particle swarm optimization (PSO), an approach is provided in [12] to determine the best location of EVCS and the optimal capacity of EVCSs for URDS. M. Dixit & R. Roy [13] proposed a method based on the Particle Swarm Optimization with the Constriction Factor technique for optimal EV placement to minimize the power losses and enhance the voltage profiles. Gurappa et al. [14] recommended the ideal location of EVCSs & DGs in RDS to reduce EV user charge, network power losses, station development cost, & DG investment. A multi-objective hybrid shuffled frog leap-teaching learning-based optimization algorithm was proposed by Battapothula et al. [15] for optimal location & sizing of FCSs to minimize voltage deviation, Cost of DG, Power losses. MSK Reddy & K.Selvajyothi [16] presented a method to identify optimal locations of the charging stations to minimize the real power losses & improve the voltage profile and reconfigure the RDS using the PSO algorithm. Ermis et al. [17] proposed artificial bee colony, wind-driven optimization & gravitational search algorithms to address the optimal power flow problem. The suggested optimization algorithms are evaluated on a conventional IEEE 9-bus power system with voltage deviation reduction, active power loss minimization, and fuel cost minimization as objective functions. M. Yesilbudak & A. Colak [18] presented the constituents, benefits, risks, projects, and standards of smart grids briefly and showed a complete literature survey on the challenges and the solutions encountered due to the addition of renewable energy sources, electric vehicles & demand-side initiatives.

According to the literature, most researchers focus on improving the placement of EVCSs/DGs for balanced RDSs. However, because the demand is dynamic, it is necessary to investigate the size and capacity of DG and the position of EVCS in URDS. In this study, the authors employed the HHO technique to identify the optimal placement and size of DG and the optimal location of EVCS in URDS. The efficiency of HHO is compared with particle swarm optimization (PSO), flower pollination algorithm (FPA), teaching-learning-based optimization (TLBO), Elephant Herding Optimization (EFO), Grasshopper Optimization Algorithm (GOA) & cuckoo search algorithm (CSA). A multi objective planning

framework is designed to determine optimal placement and sizing of EVCSs & DGs to minimize the power losses and improve the voltage profile. The simulations are performed on a standard IEEE 25-bus unbalanced test system.

2. Problem Formulation

2.1 Objective Function

The real & reactive losses are computed employing the load flow study by incorporating EVCS at optimum positions.

$$P_L(i) = \sum \left(\frac{(P_{effa}^2[i] + Q_{effa}^2[i]) * R_{aai}}{V_{ia}^2} + \frac{(P_{effb}^2[i] + Q_{effb}^2[i]) * R_{abi}}{V_{ib}^2} + \frac{(P_{effc}^2[i] + Q_{effc}^2[i]) * R_{cai}}{V_{ic}^2} \right) \quad (1) \quad [19]$$

$$Q_L(i) = \sum \left(\frac{(P_{effa}^2[i] + Q_{effa}^2[i]) * X_{aai}}{V_{ia}^2} + \frac{(P_{effb}^2[i] + Q_{effb}^2[i]) * X_{abi}}{V_{ib}^2} + \frac{(P_{effc}^2[i] + Q_{effc}^2[i]) * X_{cai}}{V_{ic}^2} \right) \quad (2) \quad [19]$$

Where, $P_{eff}[q]$ =Active power distributed beyond the bus 'q'.

$Q_{eff}[q]$ =Reactive power distributed beyond the bus 'q'.

2.2 Constraints

$$P_{supply} + \sum_{k=1}^{NG} PG_k - P_L = P_d \quad (3)$$

$$PG_k^{min} \leq PG_k \leq PG_k^{max} \quad (4)$$

$$T_k^{min} \leq T_k \leq T_k^{max}, k = 1,2,3 \dots \dots, nbus \quad (5)$$

$$0.95 \leq VG_k \leq 1.05, k = 1,2,3 \dots \dots, nbus \quad (6)$$

$$SL_k \leq SL_k^{max}, k = 1,2,3 \dots \dots, nbus \quad (7)$$

Where, P_{supply} & Q_{supply} are active & reactive power supplied
 PG_k are the active & reactive power injection from DG unit at bus 'k'

P_d & Q_d are the active & reactive power of load demand

P_L & Q_L are the active & reactive power losses

T_k is the transformer tap position

VG_k is the voltage at bus 'k'

SL is the apparent power losses.

NG is the number of generators

PG_k^{min}, PG_k^{max} are the active power output limits of DG.

T_k^{min}, T_k^{max} are the limits of the transformer tap position.

SL_k^{max} is the maximum apparent power

3. HHO for EVCS & DG Simultaneous Optimal Placement

The "surprise pounce" is the Harris hawk's primary method of catching prey. Several hawks strike from many directions while focusing on an imagined rabbit external shield. The attack can be completed quickly by grabbing an unsuspecting object in a few seconds, however depending on the target ability to flee and habits, the "surprise pounce" may

require many short-length, fast dives around the object more than a few minutes.

When the finest hawk bows down to target & becomes lost, the party members swap tactics, and one of them continues the hunt. The benefit of these supportive techniques is that the Harris hawks may chase the identified rabbit until it is exhausted, increasing its vulnerability. It will not regain its self-protective powers by distracting the escaping object. In general, HHO is divided into phases based on the “exploration” & “exploitation” of prey by Harris hawks, as well as surprise pounces and various attacking techniques.

3.1 Exploration Phase

A random position determines the hawk's position and several other hawks & is provided by eq.8. [20].

$$P(t + 1) = \begin{cases} P_k(t) - a_1|P_k(t) - 2a_2P(t)|x \geq 0.5 \\ (P_x(t) - P_m(t)) - a_3(lb + a_4(up_{lim} - lo_{lim}))x < 0.5 \end{cases} \quad (8)$$

Where P is hawk's location, P_k is the random location of a selected hawk, P_x is the point of an object, up_{lim} & lo_{lim} are the upper & lower boundaries of the study zone, a₁, a₂, a₃, a₄, and x are the arbitrary numbers in between 0 and 1. The P_m is a mean point of the current hawk's group & calculated by using eq.9.

$$P_m(t) = \frac{1}{W} \sum_{q=1}^W P_q(t) \quad (9)$$

Where P_q is qth hawk in the group & W is number of hawks.

3.2 Exploration to Exploitation

The nature of exploration may be shifted based on the intensity of the prey's escape. The intensity of the target's desire to leave can be calculated as

$$S = 2S_0(1 - \frac{t}{I}) \quad (10)$$

$$S_0 = 2n - 1 \quad (11)$$

Where I is maximum no of iterations, S₀ is initial intensity created random in between 0 & 1, and n is a random number in between 0 & 1. When S > 1, the hawks to search in different parts. Otherwise, HHO appeared to promote local searches for the finest alternatives in the area.

3.3 Exploitation Phase

The hawk's position is modified based on the following scenarios in this state.

3.3.1 Soft Besiege

This can be noticed once q ≥ 0.5 & |S| ≥ 0.5. The hawk changes its location by using eq.12.

$$P(t + 1) = \Delta P(t) - S|eP_q(t) - P(t)| \quad (12)$$

Where S is the target's absconding intensity, P_q is the location of prey, ΔP is the modification in the target location & current hawk location, and e is the diving energy. The e & ΔP are calculate by using eqs.13 & 14.

$$\Delta P(t) = P_q(t) - P(t) \quad (13)$$

$$e = 2(1 - a_5) \quad (14)$$

Where a₅ is a arbitrary number between 0 & 1.

3.3.2 Hard Besiege

This can be seen as soon as q ≥ 0.5 & |S| < 0.5. The hawk changes its location by using eq.15.

$$P(t + 1) = P_q(t) - S|\Delta P(t)| \quad (15)$$

3.3.3 Soft Besiege with Progressive Rapid Dives

This stage is take place after q < 0.5 & |S| ≥ 0.5 and hawk's new location is formed as

$$A = P_q(t) - S|\vartheta P_q(t) - P(t)| \quad (16)$$

$$C = Y + z * \text{Func}(M) \quad (17)$$

Where A & C are two freshly created hawks, ϑ is jumping strength, z is an M dimension arbitrary vector & Func is the flight function and may be calculated as

$$\text{Levy}(m) = 0.01 * \frac{\eta * \tau}{|\vartheta|^{1/\beta}} \quad (18)$$

Where η, ϑ are two arbitrary numbers and τ is defined as:

$$\tau = \left(\frac{\Gamma(1+\Upsilon) * \sin(\frac{\pi\Upsilon}{2})}{\Gamma(\frac{1+\Upsilon}{2}) * \Upsilon * 2^{\frac{\Upsilon-1}{2}}} \right)^{\frac{1}{\beta}} \quad (19)$$

Where 'Υ is equal to 1.5. The location of hawk is altered during eq 20 in this stage.

$$P(t + 1) = \begin{cases} A & \text{If } F(A) < F(P(t)) \\ C & \text{If } F(C) < F(P(t)) \end{cases} \quad (20)$$

Where F is the objective function, A & C are two results obtained from eqs16 & 17.

3.3.4 Hard Besiege with Progressive Rapid Dives

This can be seen once q < 0.5 & |S| < 0.5 and the succeeding new results are generated as

$$A = P_q(t) - S|9P_q(t) - P_m(t)| \quad (21)$$

$$C = Y + z * \text{Func}(M) \quad (22)$$

Where P_m is the median location of the hawks in present group. The status of the hawk is consequently transformed as

$$P(t + 1) = \begin{cases} A & \text{If } F(A) < F(P(t)) \\ C & \text{If } F(C) < F(P(t)) \end{cases} \quad (23)$$

3.4 Flow Chart

This section shows the chronological stages involved in determining the optimal allocation of EVCS & DGs utilizing the HHO algorithm in Figure 1 [21].

4. Results & Discussions

The proposed optimization algorithm has been evaluated using the MATLAB program, implemented in a PC with Intel Core i5-4210U processor, up to 1.7 GHz and 8 GB of RAM. The simulations are performed on IEEE 25-bus unbalanced test system. The minimum and maximum limits of active power injection by a DG are 250kW & 400kW per phase with unity power factor, respectively. The limits of active & reactive power losses are taken as $\pm 2.5\%$ of the total load. The

total power demand of EVCSs is mainly dependent on the number of charging points (CP) and their type. In this study, depending upon the type of the electric vehicle (EV) model and the number of CPs, the power demand of EVCSs is determined. The design features of CPs such as types of EVs that can charge at a time in a particular EVCS and their power ratings in kW, the minimum and maximum number of CPs for different EVs, and correspondingly the minimum and maximum power rating of CS. The details are given in Table 1.

This article offers the following summaries to address the impact of EVCSs and DGs on the system.

Case1: URDS without integrating DGs and EVCSs.

Case2: URDS with min & max CPs operated in EVCS & without integrating the DGs.

Case3: URDS with optimal integration of EVCSs with min & max CPs operated.

Case4: URDS with simultaneous allocation of DG & EVCS with min CPs operated.

Case5: URDS with simultaneous allocation of DG & EVCS with max CPs operated.

Table 1: Design features of EVCSs for the simulation [22].

EV Type	EV power rating (kW)	No. of CPs		Rating of CS (kW)	
		Min	Max	Min	Max
Chevrolet VOLT	2.2	6	15	13.2	33
CHANG-AN YIDONG	3.75	6	15	22.5	56.25
Tesla Model X	13	6	15	78	195
BMW i3	44	6	15	264	660
SAE J1772 Standard	7	6	15	42	105
Total power rating of CS (kW)		30	75	419.7	1049.25

4.1 Case 1: URDS without integrating DGs and EVCSs

Line and load data of 3- ϕ 25 bus URDS are given in [23]. A Single-line diagram of 3- ϕ 25 bus URDS is presented in Figure 2. The base load of the system in a, b & c phases are 1073.3+j792 kVA, 1083.3+j801 kVA & 1083.3+j800 kVA,

correspondingly. The minimum voltage appeared is 0.9371, 0.9381 & 0.9442 pu at bus 12, the total real power losses are 43.5924, 45.6421 & 34.3261 kW and the total reactive power losses are 49.9860, 45.5825 & 48.5777 kVAr in a, b & c phases respectively. The test system performance is given in Figure 3 & Table 2.

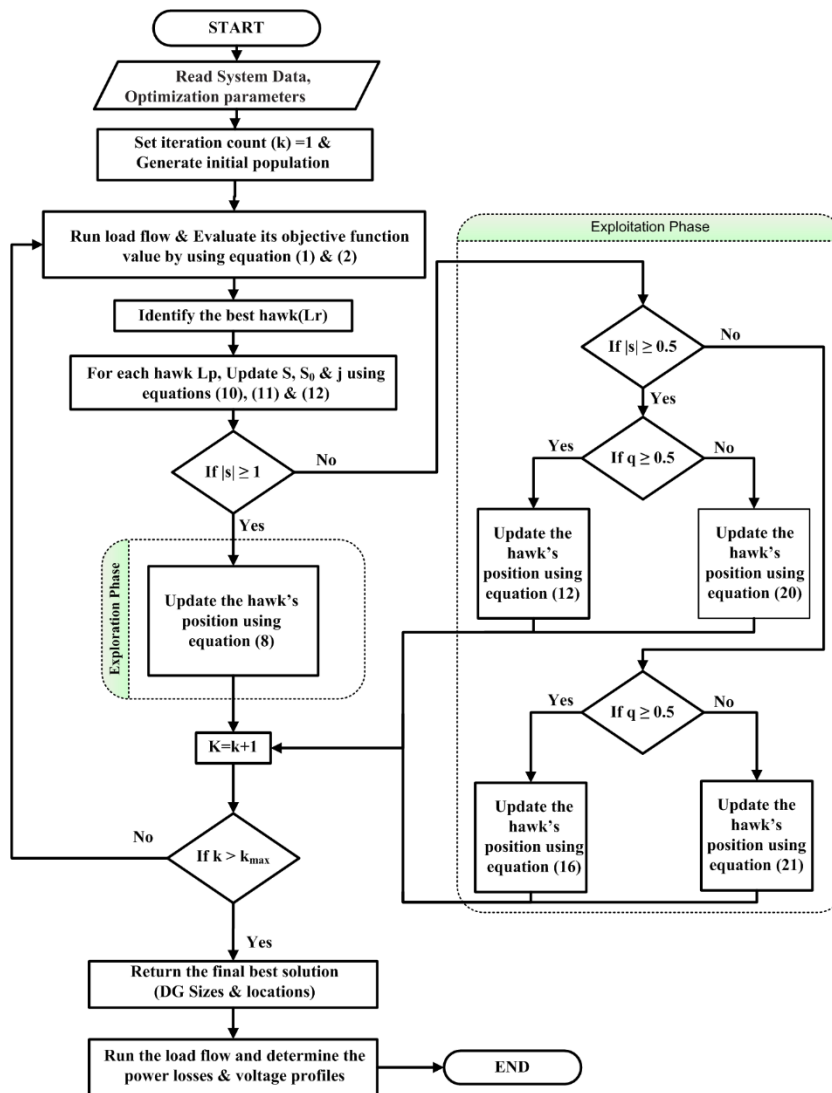


Figure 1. Flowchart of HHO Algorithm

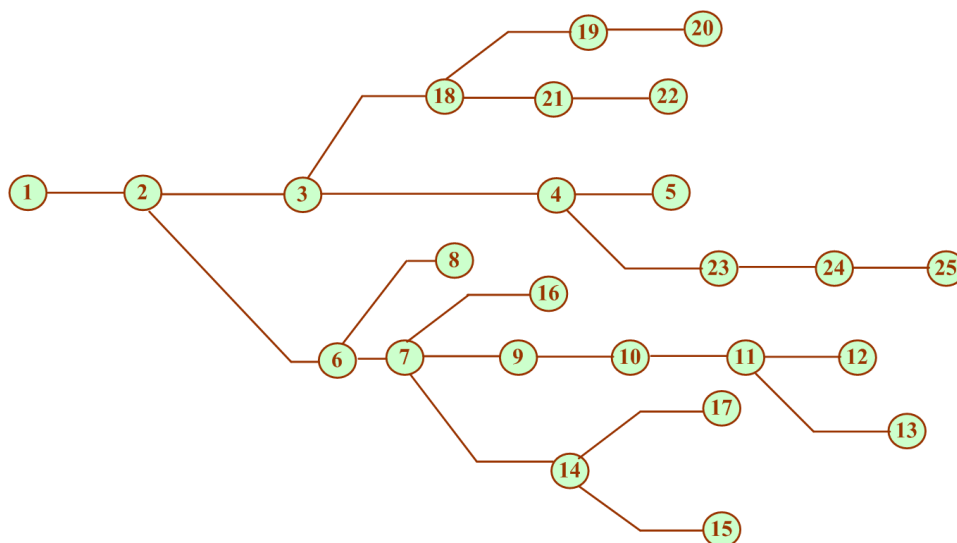


Figure 2. Single line diagram of 25 bus URDS

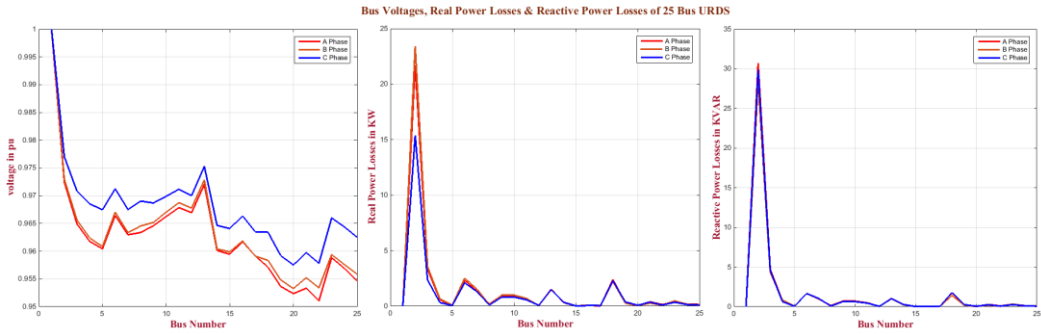


Figure 3. Bus Voltages, Real & Reactive power losses of 25 bus URDS without integrating DGs and EVCSs

4.2 Case2: URDS with min & max CPs operated in EVCS & without integrating the DGs

The total power demand when EVCS is operated with the minimum number of charging points is increased by 419.7 kW and when operated with the maximum number of charging points, it is increased by 1049.25 kW.

When minimum number of Charging Points operated in EVCS, the real power losses are increased to 54.2458, 56.7018 & 42.6423 kW, the reactive power losses are increased to 62.1327, 56.5319 & 60.2263 kVAr and the minimum voltages are decreased to 0.9305, 0.9313 & 0.9389 p.u in phase a, b & c respectively at bus 12. The test system performance is given in Table 2. When maximum number of Charging Points operated in EVCS, the real power losses are increased to 73.4256, 76.6128 & 57.5937 kW, the reactive power losses are increased to 83.9727, 76.2019 & 81.1367 kVAr and the minimum voltages are decreased to 0.9207, 0.9212 & 0.9310

p.u in phase a, b & c respectively at bus 12. The test system performance is given in Table 2.

4.3 Case3: URDS with optimal integration of EVCSs with min & max CPs operated

The optimal location is 2. The real power losses are decreased to 47.6703 kW, 49.9648 kW & 37.1916 kW, the reactive power losses are reduced to 55.7925 kVAr, 50.7819 kVAr & 54.1339 kVAr and the minimum voltage is raised to 0.9353, 0.9363 & 0.9430 p.u in phases a, b & c respectively when minimum charging points are operated at EVCS. The minimum voltage appears at bus number 12. Similarly, for the maximum number of Charging Points operated, the real power losses are decreased to 54.7319, 57.4194 & 42.1552 kW, the reactive power losses are reduced to 65.8439, 59.7626 & 63.7137 kVAr and the minimum voltage is raised to 0.9327, 0.9335 & 0.9412 p.u in phase a, b & c respectively. The minimum voltage appears at bus number 12. The test system performance is given in Table 2.

Table 2: System performance with minimum & maximum EVCSs & without integrating the DGs.

Case No. Loading Condition	Ploss (kW)			Qloss (kVAr)			Vmin (p.u)		
	A-Ph	B-Ph	C-Ph	A-Ph	B-Ph	C-Ph	A-Ph	B-Ph	C-Ph
1. Without EVCS load	43.5924	45.6421	34.3261	49.9860	45.5825	48.5777	0.9371	0.9381	0.9442
2(a). With minimum EVCS load (without optimal placement)	54.2458	56.7018	42.6423	62.1327	56.5319	60.2263	0.9305	0.9313	0.9389
2(b). With maximum EVCS load (without optimal placement)	73.4256	76.6128	57.5937	83.9727	76.2019	81.1367	0.9207	0.9212	0.9310
3(a). Optimal integration of EVCS load at bus no 2 With minimum EVCS load	47.6703	49.9648	37.1916	55.7925	50.7819	54.1339	0.9353	0.9363	0.9430
3(b). Optimal integration of EVCS load at bus no 2 With maximum EVCS load	54.7319	57.4194	42.1552	65.8439	59.7626	63.7137	0.9327	0.9335	0.9412

4.4 Case4: URDS with simultaneous allocation of DG & EVCS with min CPs operated

The optimum location of the EVCS is 2, whereas DG is 13. The DG size is 275.4839, 272.6971 & 281.2739 kW, the

real power losses are 34.3016, 36.1581 & 26.6349 kW and the reactive power losses are 40.7973, 37.5192 & 39.4162 kVAR in phases a, b & c respectively. The minimum voltages are identified as 0.9522, 0.9547 & 0.9584 per unit in phases a, b & c correspondingly. The test system performance is given in Table 3 & Figure 4.

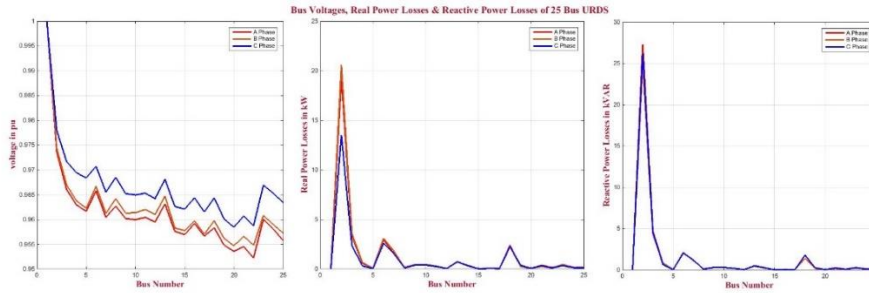


Figure 4. Bus Voltages, Real & Reactive power losses of 25 bus URDS with simultaneous allocation of DG & EVCS with minimum CPs operated

4.5 Case5: URDS with simultaneous allocation of DG & EVCS with max CPs operated.

The optimum location of the EVCS is 2, whereas DG is 13. The DG size is 388.9737, 380.2428 & 383.5937 kW , the

real power losses are 38.2326, 40.3281 & 29.6954 kW and the reactive power losses are 45.2218, 41.8251 & 44.0279 kVAR, minimum voltages are identified as 0.9510, 0.9533 & 0.9575 pu in phases a, b & c respectively. The test system performance is given in Table 3 & Figure 5.

Table 3: System performance with optimal integration of DG & EVCS With min & max CPs operated

Description	Case-4			Case-5		
	Ph-A	Ph-B	Ph-C	Ph-A	Ph-B	Ph-C
DG Size(kW)	275.4839	272.6971	281.2739	388.9737	380.2428	383.5937
Total DG Size(kW)	829.4549			1152.8102		
DG place (Bus Number)	13			13		
EVCS location	2			2		
Real Power Loss (kW)	34.3016	36.1581	26.6349	38.2326	40.3281	29.6954
Total Real Power Losses (kW)	97.0946			108.2561		
Reactive Power Loss (kVAR)	40.7973	37.5192	39.4162	45.2218	41.8251	44.0279
Total Reactive Power Losses (kVAR)	117.7327			131.0748		
Minimum Voltage	0.9522	0.9547	0.9584	0.951	0.9533	0.9575

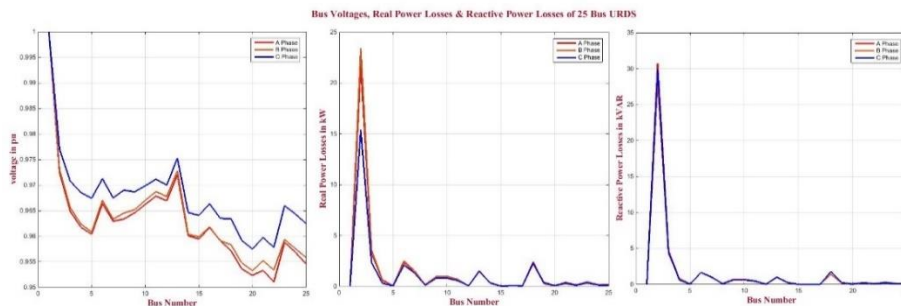


Figure 5. Bus Voltages, Real & Reactive power losses of 25 bus URDS with simultaneous allocation of DG & EVCS with maximum CPs operated

5. Comparison of HHO algorithm with other metaheuristic algorithms

The outcomes of HHO for Case-5 are related with other metaheuristic algorithms, like, PSO [24], FPA [25], TLBO [26], EFO [27], GOA [28] & CSA [29]. In HHO the number of hawk’s i.e. population size, is set to 10. During a run in PSO, the inertia factor’s range is reduced linearly from 0.8 to 0.5. The social & cognitive coefficients are treated equally. The switching parameter in CSA is fixed at 0.8. The teaching factor in TLBO can be either 1 or 2 at random. In EHO, $\alpha=0.5$, $\beta=0.1$, popsize=100, Maxgen=60. For GOA, strength of attraction & the gauge distance are 0.6 & 1.6. For all methods, number of iterations = 100, search variables = 9 (i.e., 1DG

location, 1DG size & 1 EVCS for each phase). The lower & upper boundaries for location = (2, n bus) & DG sizes = (0,400).

To test the resilience of HHO in addressing optimization issues, each method was simulated for 50 separate runs for Case 5. HHO can be considered a more reliable & effective procedure than other commonly used procedures. Table 4 shows the comparative investigation of losses & voltages for the cases considered, while Table 5 shows the best result produced by all methods after 50 separate run simulations and the average computing time. Figure 6 depicts the convergence features of multiple methods for case 4.

Table 4: Comparative investigation of losses & voltages of 25 bus URDS for different cases considered

Scenarios	Active power losses(kW)			Reactive power losses(kVAr)			Min.Voltage(pu)		
	A	B	C	A	B	C	A	B	C
Case-1: Without integrating DGs and EVCSs	43.5924	45.6421	34.3261	49.9860	45.5825	48.5777	0.9371	0.9381	0.9442
Case-2(a) : Minimum CPs operated in EVCS (without DG)	54.2458	56.7018	42.6423	62.1327	56.5319	60.2263	0.9305	0.9313	0.9389
% Increase (↑)/ Decrease (↓) w.r.t base case	↑24.44	↑24.23	↑24.23	↑24.30	↑24.02	↑23.98	↓0.70	↓0.72	↓0.56
Case-2(b): Maximum CPs operated in EVCS (without DG)	73.4256	76.6128	57.5937	83.9727	76.2019	81.1367	0.9207	0.9212	0.9310
% Increase (↑)/ Decrease (↓) w.r.t base case	↑68.44	↑67.86	↑67.78	↑67.99	↑67.17	↑67.02	↓1.75	↓1.80	↓1.40
Case-3(a): Optimal integration of EVCS with minimum CPs operated (without DG)	47.6703	49.9648	37.1916	55.7925	50.7819	54.1339	0.9353	0.9363	0.9430
% Increase (↑)/ Decrease (↓) w.r.t case-2(a)	↓12.12	↓11.88	↓12.78	↓10.20	↓10.17	↓10.11	↑0.52	↑0.54	↑0.44
Case-3(b): Optimal integration of EVCS with maximum CPs operated (without DG)	54.7319	57.4194	42.1552	65.8439	59.7626	63.7137	0.9327	0.9335	0.9412
% Increase(↑)/ Decrease (↓) w.r.t case-2(b)	↓25.46	↓25.05	↓26.81	↓21.59	↓21.57	↓21.47	↑1.30	↑1.34	↑1.09
Case-4: Simultaneous allocation of DG & EVCS with minimum CPs operated	34.3016	36.1581	26.6349	40.7973	37.5192	39.4162	0.9522	0.9547	0.9584
% Increase (↑)/ Decrease (↓) w.r.t case-2(a)	↓36.77	↓36.23	↓37.54	↓34.34	↓33.63	↓34.55	↑2.33	↑2.51	↑2.08
Case-5: Simultaneous allocation of DG & EVCS with maximum CPs operated	38.2326	40.3281	29.6954	45.2218	41.8251	44.0279	0.9510	0.9533	0.9575
% Increase (↑)/ Decrease (↓) w.r.t case-2(b)	↓47.93	↓47.36	↓48.44	↓46.15	↓45.11	↓45.74	↑3.29	↑3.48	↑2.85

Table 5: Evaluation of best solution obtained by metaheuristic algorithms for case 5

Algorithm	Phase	DG Size in kW, bus	EVCS location	Ploss(kW)	Qloss(kVAr)	Vmin(pu)	Time(s)
HHO	A	388.9737, 13	2	38.2326	45.2218	0.951	1.1752
	B	380.2428, 13	2	40.3281	41.8251	0.9533	
	C	383.5937, 13	2	29.6954	44.0279	0.9575	
PSO	A	410.8975, 13	2	40.1258	46.5721	0.9483	1.6549
	B	421.5671, 13	2	42.1985	42.5423	0.9493	
	C	398.2687, 13	2	30.2547	44.8549	0.9569	
FPA	A	408.2369, 13	3	39.2567	46.4268	0.9496	1.5942
	B	410.2374, 13	3	41.9546	42.1472	0.9511	
	C	395.6421, 13	3	30.1157	44.3571	0.9569	
TLBO	A	398.2387, 13	2	39.8425	46.3265	0.9497	1.2987
	B	389.2567, 13	2	40.9624	41.9953	0.9521	
	C	388.3486, 13	2	29.8869	44.0863	0.9572	
EFO	A	401.8934, 14	2	39.1204	46.4934	0.9484	1.3281
	B	399.9986, 14	2	41.0251	42.0048	0.9528	
	C	392.1574, 14	2	30.2347	44.1473	0.9567	
GOA	A	411.8532, 13	2	39.0215	46.4856	0.9489	1.2874
	B	419.3286, 13	2	40.9698	42.3172	0.9517	
	C	396.2381, 13	2	30.4783	44.1937	0.9571	
CSA	A	399.9832, 13	2	38.9569	45.5124	0.9504	1.2175
	B	388.2314, 13	2	40.4587	41.8998	0.9514	
	C	380.9856, 13	2	29.9967	44.0863	0.9568	

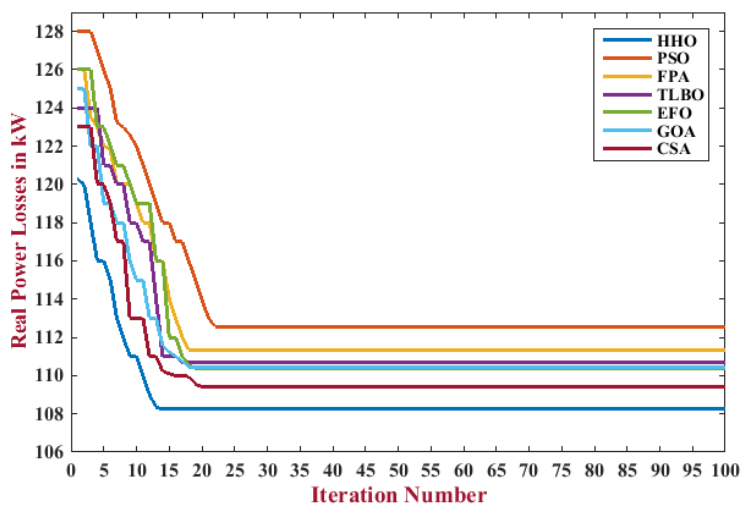


Figure 6. Convergence characteristics of various algorithms for case-5 in the 25-bus URDS

6. Conclusion

EVs are the future of transport for conquering carbon emissions, leading to the formation of charging stations. As a result, EVCSs will become an unavoidable element of the distribution grid. Including EVCSs in URDS increases the system losses and a significant voltage variation at remote buses. Hence, the introduction of DGs is required to reduce URDS losses & improve the voltage profile when charging EVs with EVCSs. The influence of incorporating EVCSs & DGs into URDS is investigated in this work by utilizing a modified forward-backward load flow.

The following findings demonstrate the effectiveness & advantages of the proposed framework. The planning framework is to determine the optimal EVCS placement & DG capacity & placement, aiming to lower power loss and voltage variation. For the effective placement of EVCSs and DGs in the distribution network, the HHO method is utilized. The efficiency of the suggested method is evaluated on 25 bus URDS.

With the inclusion of EVCSs with minimum CPs operated and without placing them at optimized location, the real power losses are increased by 24.44%, 24.23% & 24.23%, reactive power losses are increased by 24.30%, 24.02% & 23.98% & the minimum voltage is reduced by 0.70%, 0.72% & 0.56% in A,B & C phases respectively. By placing the EVCS at optimum location i.e. at bus no 2, the real power losses are reduced by 12.12%, 11.88% & 12.78%, reactive power losses are reduced by 10.20%, 10.17% & 10.11% & the minimum voltage is improved by 0.52%, 0.54% & 0.44% in A, B & C phases respectively when compared to EVCSs with minimum CPs operated and without placing them at optimized location. With the inclusion of EVCSs with maximum CPs operated and without placing them at optimized location, the real power losses are increased by 68.44%, 67.86% & 67.78%, reactive power losses are increased by 67.99%, 67.17% & 67.02% & the minimum voltage is reduced by 1.75%, 1.80% & 1.40% in A,B & C phases respectively. By placing the EVCS at optimum location i.e. at bus no 2, the real power losses are reduced by 25.46%, 25.05% & 26.81%, reactive power losses are reduced by 21.59%, 21.57% & 21.47% & the minimum voltage is improved by 1.30%, 1.34% & 1.09% in A, B & C phases respectively when compared to EVCSs with maximum CPs operated and without placing them at optimized location.

With the optimal integration of DG at bus 13 & EVCS at bus 2 with minimum number of CPs operated, the real power losses are reduced by 36.77%, 36.23% & 37.54%, reactive power losses are reduced by 34.34%, 33.63% & 34.55% & the minimum voltage is improved by 2.33%, 2.51% & 2.08% in A, B & C phases respectively when compared to EVCSs with minimum CPs operated and without placing them at optimized location. With the optimum integration of DG & EVCS with

maximum number of CPs operated, the real power losses are reduced by 47.93%, 47.36% & 48.44%, reactive power losses are reduced by 46.15%, 45.11% & 45.74% & the minimum voltage is improved by 3.29%, 3.48% & 2.85% in A, B & C phases respectively when compared to EVCSs with maximum CPs operated and without placing them at optimized location. The suggested HHO has the lowest objective function when compared to other optimization techniques. HHO has demonstrated its advantage in terms of robustness and consistency in a statistical study based on 50 unique run time data. Finally, in handling the nonlinear and complicated optimization problem, HHO outperformed other metaheuristic algorithms. It is recognized that HHO manifests fast convergence features. In future research activity, the optimization problem can be continued for a hybrid DG system with different DG units, including battery storage. Furthermore, the impact of renewable DG's intermittent nature may be handled using uncertainty modelling.

References

- [1] D. Sanchari, Kari Tammi, Karuna Kalita, Pinakeshwar Mahanta, "Impact of Electric Vehicle Charging Station Load on Distribution Network", *Energies*, 11, no. 1:178, 2018. DOI: <https://doi.org/10.3390/en11010178>. (Article)
- [2] A. Mohsenzadeh, Samaneh Pazouki, Shahab Ardalan & Mahmoud Reza Haghifam, "Optimal placing and sizing of parking lots including different levels of charging stations in electric distribution networks", *International Journal of Ambient Energy*, 2017, DOI: 10.1080/01430750.2017.1345010. (Article)
- [3] T.Ramana, V.Ganesh & S.Sivanagaraju, "Distributed Generator Placement and Sizing in Unbalanced Radial Distribution System", *Cogeneration & Distributed Generation Journal*, Vol. 25, No. 1, 2010, pp.52-71. DOI: <https://doi.org/10.1080/15453661009709862>. (Article)
- [4] V.Janamala, U.Kamal Kumar & TKS.Pandiraju, "Future search algorithm for optimal integration of distributed generation and electric vehicle fleets in radial distribution networks considering techno-environmental aspects", *SN Appl.Sci.*, 464, 2021. DOI: <https://doi.org/10.1007/s42452-021-04466-y>. (Article)
- [5] R. Sanjay, T. Jayabarathi, T. Raghunathan, V. Ramesh & N.Mithulananthan, "Optimal Allocation of Distributed Generation Using Hybrid Grey Wolf Optimizer", *IEEE Access*, Vol. 5, 2017, pp. 14807-14818. DOI: <https://doi.org/10.1109/ACCESS.2017.2726586>. (Article)
- [6] I. A. Quadri, S. Bhowmick & D. Joshi, "A comprehensive technique for optimal allocation of distributed energy resources in radial distribution systems", *Applied Energy*, Vol. 211, 2018, pp. 1245-1260. DOI: <https://doi.org/10.1016/j.apenergy.2017.11.108>. (Article)
- [7] S. Kayalvizhi, D.M. Vinod Kumar, "Optimal planning of active distribution networks with hybrid distributed energy resources using grid-based multi-objective harmony search

- algorithm", *Applied Soft Computing*, Vol. 67, 2018, pp. 387-398. DOI: <https://doi.org/10.1016/j.asoc.2018.03.009>. (Article)
- [8] A. Jabbarly & Hossein Shayeghi, "Smart Imposing of Operational Limits in Optimizing the Technical and Economic Indexes of Distribution Network in Presence of Distributed Generation Sources", *International Journal of Ambient Energy*, 2018, DOI: 10.1080/01430750.2018.1492451. (Article)
- [9] A. Hajimiragha, CA. Canizares, MW. Fowler and A. Elkamel, "Optimal Transition to Plug-In Hybrid Electric Vehicles in Ontario, Canada, Considering the Electricity-Grid Limitations", *IEEE Transactions on Industrial Electronics*, vol. 57, no. 2, 2010, pp. 690-701. DOI: <https://doi.org/10.1109/TIE.2009.2025711>. (Article)
- [10] M.Etezadi-Amoli, K. Choma, and J. Stefani, "Rapid-Charge Electric-Vehicle Stations", *IEEE Transactions on Power Delivery*, vol. 25, no.3, pp. 1883-1887, 2010. DOI: <https://doi.org/10.1109/TPWRD.2010.2047874>. (Article)
- [11] F. Xu, G. Q. Yu, L. F. Gu, and H. Zhang, "Tentative analysis of layout of electrical vehicle charging stations", *Proceeding of East China Electric Power*, vol. 37, no. 10, 2009, pp.1677–82. (Conference Paper)
- [12] M. Satish Kumar Reddy & K. Selvajyothi, "Optimal placement of electric vehicle charging station for unbalanced radial distribution systems", *Energy Sources, Part A: Recovery, Utilization, and Environmental Effects*, 2020. DOI: <https://doi.org/10.1080/15567036.2020.1731017>. (Article)
- [13] M. Dixit, R. Roy, "PSO-CFA based optimal placement of EVs in radial distribution network for loss minimization," 2015 IEEE International Conference on Electrical, Computer and Communication Technologies (ICECCT), Coimbatore, March 5-7, 2015, pp.1-5. DOI: <https://doi.org/10.1109/ICECCT.2015.7225983>. (Conference Paper)
- [14] G. Battapothula, Y. Chandrasekhar & M. Sydulu, "Multi-objective simultaneous optimal planning of electrical vehicle fast charging stations and DGs in distribution system", *Journal of Modern Power Systems and Clean Energy*, Vol. 7, 2019, pp. 923–934. DOI: <https://doi.org/10.1007/s40565-018-0493-2>. (Article)
- [15] G. Battapothula, C. Yammani & S. Maheswarapu, "Multiobjective optimal planning of FCSs and DGs in distribution system with future EV load enhancement", *IET Electrical Systems in Transportation*, Vol. 9, No. 3, 2019, pp. 128-139. DOI: <https://doi.org/10.1049/iet-est.2018.5066>. (Article)
- [16] M. S. K. Reddy, K. Selvajyothi, "Optimal Placement of Electric Vehicle Charging Stations in Radial Distribution System along with Reconfiguration", 2019 IEEE 1st International Conference on Energy, Systems and Information Processing (ICESIP), Chennai, July 4-6, 2019, pp. 1-6. DOI: <https://doi.org/10.1109/ICESIP46348.2019.8938164>. (Conference Paper)
- [17] S. Ermis, M. Yesilbudak and R. Bayindir, "Optimal Power Flow Using Artificial Bee Colony, Wind Driven Optimization and Gravitational Search Algorithms", 2019, 8th International Conference on Renewable Energy Research and Applications (ICRERA), 2019, pp. 963-967, DOI: <https://doi.org/10.1109/ICRERA47325.2019.8996559>. (Conference Paper)
- [18] M. Yesilbudak & A. Colak, "Integration Challenges and Solutions for Renewable Energy Sources, Electric Vehicles and Demand-Side Initiatives in Smart Grids", 2018 7th International Conference on Renewable Energy Research and Applications (ICRERA), 2018, pp. 1407-1412, DOI: <https://doi.org/10.1109/ICRERA.2018.8567004>. (Conference Paper)
- [19] P. V. K. Babu and K. Swarnasri, "Adaptive PSO Technique for Optimal Placement and Sizing of DG in 3-Phase Unbalanced Radial Secondary Distribution System," 2019 IEEE International Conference on Intelligent Systems and Green Technology (ICISGT), Visakhapatnam, India, 2019, pp. 85-854, DOI: <https://doi.org/10.1109/ICISGT44072.2019.00034>. (Conference Paper)
- [20] A. A. Heidari, Seyedali Mirjalili, Hossam Faris, Ibrahim Aljarah, Majdi Mafarja & Huiling Chen, "Harris hawks optimization: Algorithm and applications", *Future Generation Computer Systems*, Vol. 97, 2019, pp. 849-872. DOI: <https://doi.org/10.1016/j.future.2019.02.028>. (Article)
- [21] P. V. K. Babu and K. Swarnasri, "Optimal integration of different types of DGs in radial distribution system by using Harris hawk optimization algorithm", *Cogent Engineering*, vol.7, no. 1, 2020. DOI: <https://doi.org/10.1080/23311916.2020.1823156>. (Article)
- [22] P. V. K Babu and K. Swarnasri, " Multi-Objective Optimal Allocation of Electric Vehicle Charging Stations in Radial Distribution System Using Teaching Learning Based Optimization", *International Journal of Renewable Energy Research*, Vol. 10, No.1, pp. 366–377, 2020. (Article)
- [23] P. V. K. Babu, K. Swarnasri, P. Vijetha, "A three phase unbalanced power flow method for secondary distribution system", *Advances in Modelling and Analysis B*, Vol. 61, No. 3, pp. 139-144, 2018. DOI: https://doi.org/10.18280/ama_b.610306. (Article)
- [24] J. Kennedy, RC. Eberhart, "Particle swarm optimization", In: *Proceedings of IEEE International Conference on Neural Networks*, Perth, Australia, vol 4., 1995, pp 1942–1948. DOI: <https://doi.org/10.1109/ICNN.1995.488968>. (Conference Paper)
- [25] XS. Yang, "Flower pollination algorithm for global optimization", In: *International conference on unconventional computing and natural computation*.

- Springer, Berlin, Heidelberg, 2012. DOI: 157:93–109,2008. DOI:
https://doi.org/10.1007/978-3-642-32894-7_27.
(Conference Paper) <https://doi.org/10.1140/epjst/e2008-00633-y>. (Article)
- [26] RV. Rao, VJ. Savsani, DP. Vakharia, “Teaching–learning-based optimization: a novel method for constrained mechanical design optimization problems”, *Comput Aided Des* 43(3):303–315, 2011. DOI: <https://doi.org/10.1016/j.cad.2010.12.015> (Article)
- [27] C.H. Prasad, K. Subbaramaiah, & P. Sujatha, “Cost–benefit analysis for optimal DG placement in distribution systems by using elephant herding optimization algorithm”, *Renewables: Wind, Water and Solar*, 6(1), 2019. DOI: <https://doi.org/10.1186/s40807-019-0056-9>. (Article)
- [28] CM. Topaz, AJ. Bernoff, S. Logan, W. Toolson, “A model for rolling swarms of locusts”, *Eur Phys J Spec Top*
- [29] XS. Yang, S. Deb, “Cuckoo search via Lévy flights”, In: *Proceedings of world congress on nature and biologically inspired computing*. IEEE Publications, USA, 2008, pp 210–214. DOI: <https://doi.org/10.1109/NABIC.2009.5393690>. (Article)
- [30] F. K. V. Junior, B. A. Teplaira, M. C. Franklin, "Optimal Reliability of a Smart Grid", *International Journal of Smart Grid*, Vol.5, No.2, June, 2021. (Article)
- [31] M. Gilbert, N. Shililiandumi, H Kimaro, "Evolutionary Approaches to Fog Node Placement in LV Distribution Networks", *International Journal of Smart Grid*, Vol.5, No.1, March, 2021. (Article)